Fluid and kinetic structure of magnetic merging in the Swarthmore Spheromak Experiment

W. H. Matthaeus
Bartol Research Institute, University of Delaware, Newark, Deleware, USA

C. D. Cothran, M. Landreman, and M. R. Brown
Department of Physics and Astronomy, Swarthmore College, Swarthmore, Pennsylvania, USA

Received 1 July 2005; revised 27 September 2005; accepted 26 October 2005; published 6 December 2005.

[1] Measurement of the in-plane Lorentz force and the out-of-plane magnetic field associated with the Hall electric field near the reconnection zone in the Swarthmore Spheromak Experiment (SSX) confirms expectations, based on simulation, theory and spacecraft data, that the quadrupolar out-of-plane magnetic field is a signature of collisionless effects in magnetic reconnection with a weak guide field. **Citation:** Matthaeus, W. H., C. D. Cothran, M. Landreman, and M. R. Brown (2005), Fluid and kinetic structure of magnetic merging in the Swarthmore Spheromak Experiment, *Geophys. Res. Lett.*, *32*, L23104, doi:10.1029/2005GL023973.

1. Introduction

[2] Magnetic reconnection involves topological changes of the magnetic field and characteristic activity in and around a reconnection zone. Distinctive features include concentration of electric current density, characteristic plasma flows, and ion heating; these are expected theoretically [*Priest and Forbes*, 2000; *Sonnerup*, 1979], simulated [e.g., *Shay et al.*, 1998] and observed in the laboratory [e.g., *Hsu et al.*, 2000]. Many of these features are also observed through model dependent interpretations of spacecraft data [e.g., *Phan et al.*, 2000]. It is the aim of this paper to further corroborate theoretical expectations of Hall effects in collisionless reconnection and to thereby complement spacecraft investigations of the same phenomena [e.g., *Wygant et al.*, 2005].

[3] The baseline description of reconnection in terms of resistive, single fluid magnetohydrodynamics (MHD), is incomplete [*Biskamp et al.*, 1995] in low collisionality plasmas encountered in space, astrophysical and laboratory settings. In such cases, at scales on the order of the ion inertial length c/ω_{pi}, or smaller, kinetic effects become evident, and a more complete representation is required [*Biskamp et al.*, 1995; *Ma and Bhattacharjee*, 1996; *Shay et al.*, 1998]. A substantial Hall effect contribution to Ohm's law indicates a differential flow of electrons and ions, and decoupling of the magnetic field from the ion fluid motion. The magnetic field, remaining almost frozen-in the electron fluid, is deflected in the direction antiparallel to the electric current density, and reconnection becomes inherently three dimensional (3D). Special note has been made of the quadrupolar out-of-plane magnetic field near the reconnection zone, a 3D feature associated with the Hall effect [*Sonnerup*, 1979; *Terasawa*, 1983]. This has been interpreted in simulations [*Shay et al.*, 1998] and space observations [*Oieroset et al.*, 2001; *Mozer et al.*, 2002; *Scudder et al.*, 2002] as a signature of non-MHD kinetic reconnection physics. Controlled laboratory plasma experiments can identify these kinetic signatures of reconnection, and are independent of the assumptions usually made in simulations or spacecraft data interpretation. Here, using the Swarthmore Spheromak Experiment (SSX), we describe the out-of-plane quadrupolar magnetic field associated with a strong Hall effect term within a few c/ω_{pi} of the merging region, and the in-plane Hall electric field, that generates the out-of-plane magnetic field.

2. Spheromak Reconnection Experiments

[4] SSX studies reconnection between two interacting spheromaks [*Brown*, 1999]. The present work complements earlier SSX study of current filamentation, topological changes in magnetic field [*Cothran et al.*, 2003] and production of energetic particles [*Brown et al.*, 2002]. Complementary results from the Princeton MRX device describe reconnection rates, anomalous resistivity and other properties of reconnection [*Yamada et al.*, 1997a, 1997b; *Ji et al.*, 1998].

[5] In SSX, two coaxial magnetized plasma guns produce fully ionized spheromak plasmas within separate cylindrical copper flux conservers (perfectly conducting on the timescale of the experiment); see Figure 1. Cut-out sectors at the midplane allow interaction of the two spheromaks and define the region of reconnection. Each flux conserver diameter is 50 cm; the Alfvén crossing time of this distance is ≈ 3 μs. SSX plasmas are characterized by 20 eV temperatures and $1 \times 10^{14}/\mathrm{cm}^3$ density. SSX plasmas are in the MHD regime, as $\rho_i \approx 1$ cm is small, and $S \approx 1000$, and are weakly collisional, having ion mean free path $\lambda_{ii} \approx 5$ cm, and $\omega_{ci}\tau_{ii} \approx 6$.

[6] Each plasma gun can selectively produce a nearly force-free spheromak of either sign of magnetic helicity (designated L or R for left- or right-handed.) LR or counter-helicity interaction produces the most robust reconnection activity [*Kornack et al.*, 1998; *Brown*, 1999; *Lukin et al.*, 2001].

3. Magnetic Diagnostics and Properties

[7] In LR mode, the SSX guns eject the spheromaks at time $t \approx 20$ μs, and an initial driven phase of reconnection

0094-8276/05/2005GL023973$05.00

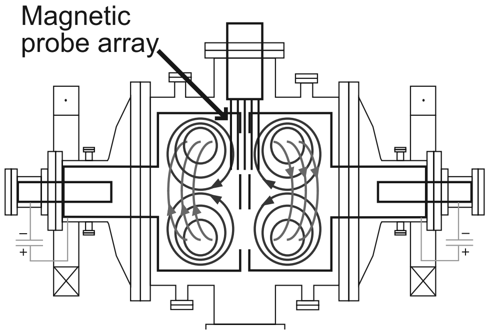

Figure 1. Diagram of the SSX device showing the location of the magnetic probe array.

lasts until $t \approx 50$ μs. Subsequently, weakly driven or spontaneous reconnection persists for tens of Alfvén crossing times [*Lukin et al.*, 2001].

[8] To analyze three-dimensional magnetic properties in the reconnection region, SSX employs an array [*Landreman et al.*, 2003] of 25 linear probes, each containing a triplet of B-dot (pick-up) coils at eight locations, for a total of 200 vector **B** measurements on a $5 \times 5 \times 8$ lattice. The full probe array is sampled every 0.8 μs, thus resolving MHD fluctuations. The ≈2 cm lattice spacing resolves the ion inertial scale c/ω_{pi}, computed from the nominal density. The measurement error is 20 G in each field component.

[9] Figure 2 illustrates magnetic data from the merging region. The 3D data are projected onto a plane (determined by inspection) in which the magnetic field most closely resembles a standard 2D X-type reconnection model. This plane is canted relative to the direction of spheromak encounter due to the twist in each flux tube associated with the toroidal and poloidal field components. The data shown are from the spontaneous reconnection phase of an LR merging experiment at time $t = 64$ μs. This discharge will be discussed below, but we draw the same conclusions upon analysis of 36 such "shots" and their average.

[10] To our knowledge, the SSX experimental setup is unique in its ability to measure space and time derivatives of the magnetic field, its 3D structure [*Cothran et al.*, 2003] and the reconstruction of several nonideal terms (except electron pressure) in the generalized Ohm's law [*Cothran et al.*, 2005]. We now use the experimental capability of measuring $\mathbf{J} = c/4\pi\nabla \times \mathbf{B}$ as well as $\mathbf{J} \times \mathbf{B}$ from the magnetic field probe data, to examine kinetic signatures in the reconnection zone.

4. Kinetic and Fluid Magnetic Signatures

[11] In the usual scenario for magnetic reconnection, strong magnetic shear leads to a concentration of electric current density in the reconnection zone. To verify that a current channel coexists with the field reversal (Figure 2), we illustrate (Figure 3) the out-of-plane component of current density. One can see that a strong localized current enhancement at $t = 32$ μs and that the current channel has weakened by $t = 64$ μs. Earlier SSX results showed additional evidence of MHD scale reconnection [*Kornack et al.*, 1998; *Qin et al.*, 2001; *Brown et al.*, 2002].

[12] Most of the energy in the SSX spheromaks is in structures with scale ≈50 cm, while the current channel (Figure 3) has a scale of 2 to 4 cm (1–2 probe spacings) at $t = 32$ μs, comparable to $c/\omega_{pi} \approx 2$ cm estimated from electron density measurements [*Kornack et al.*, 1998]. These conditions favor investigation of the expected transition between fluid and kinetic behavior in this region.

[13] In Figure 2 the isosurfaces illustrate the out-of-plane magnetic field component (again defined as normal to the 2D-like X-point plane.) There is a clear quadrupolar structure to the out-of-plane magnetic field, as predicted on theoretical grounds by *Sonnerup* [1979] for collisionless reconnection. The interpretation is that the measured quadrupolar magnetic field having a magnitude of 100–150 Gauss is a consequence of the circulation of the Hall effect electric field $\mathbf{E}_{Hall} = \frac{1}{ne}\mathbf{J} \times \mathbf{B}$. This term comes into prominence when current sheets thin to $\sim c/\omega_{pi}$, and is a characteristic kinetic signature of reconnection in the low collisionality regime [*Sonnerup*, 1979; *Shay et al.*, 1998].

[14] The quadrupolar field is seen on the wings of the electric current concentration, as expected according to the following argument. The current concentration has strength $J_z \propto \omega_{pi} B_{2D}/c$ in the out-of-plane z direction for in-plane magnetic field B_{2D}. The Hall contribution to the out-of-plane component of $\partial\mathbf{B}/\partial t$ is of order $\hat{z} \cdot \nabla \times (\mathbf{J} \times \mathbf{B}) \sim \mathbf{B} \cdot \nabla J_z$, which is readily verified to exhibit a quadrupole signature under the assumed conditions. In SSX there is a weak self-generated "guide" field of strength ≈80 G at the nominal X-point region (see Figure 2) near $x = 0$ [*Cothran et al.*, 2003]. This distorts the symmetry [*Wang et al.*, 2000] of the out-of-plane quadrupole.

[15] Figure 2 provides a level of evidence for the Hall effect-induced quadrupolar magnetic field that is compa-

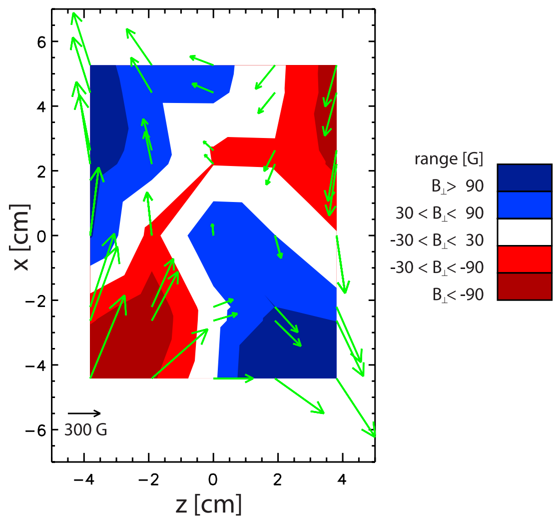

Figure 2. Magnetic field vectors in the reconnection zone depicted in a plane selected to be as close as possible to the idealized 2D reconnection geometry. X-point configuration is evident, at time $t = 64$ μsec, when spontaneous reconnection is ongoing. The scale is indicated by a vector of magnitude 300 G in the lower left corner. Superposed is a color map of the out-of-plane component of the magnetic field, exhibiting a quadrupolar pattern (positive, blue in upper left and lower right; negative, red, in lower left and upper right) which reaches a magnitude of 100 to 150 Gauss near the outer edges of the probe array.

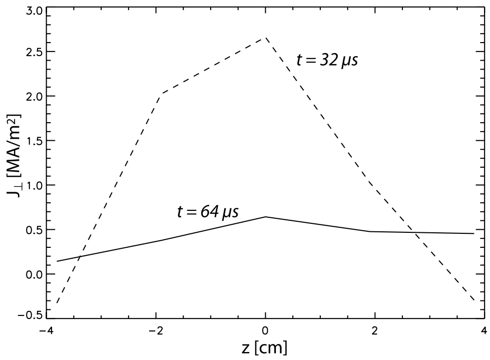

Figure 3. Profile of out-of-plane electric current density (MA/m^2) at two times in the discharge, t = 32 μs and t = 64 μs, both relative to the plane shown in Figure 2, and at x = 2 cm. At t = 32 μs, a current channel is evident with half width about a probe spacing $\approx c/\omega_{pi}$, and a maximum value ≈ 2 MA/m^2. At t = 64 μs, the same time as data in Figures 2 and 4, the current channel is broader than the probe array, with values around 0.5 MA/m^2.

rable to evidence reported in spacecraft measurements of reconnection regions in the terrestrial magnetosphere [*Oieroset et al.*, 2001; *Mozer et al.*, 2002]. Like those cases, the quadrupolar field is accompanied by other signatures of reconnection – here, the current channel (see Figure 3), global topological change of the magnetic field, and production of energetic particles [*Brown et al.*, 2002].

[16] We seek to provide further confirmation that the Hall electric field is generating the observed quadrupolar out-of-plane magnetic field. To this end, we estimate the total electric field, and directly measure $\mathbf{J} \times \mathbf{B}/(ne)$, thus characterizing the driver of the quadrupolar magnetic field.

[17] The out-of-plane magnetic field is predicted to occur [*Sonnerup*, 1979] due to contributions by $\mathbf{E}_{Hall}$. Now we show that this Hall electric field is both strong enough, and of the requisite spatial structure, to be identified as the generator of the quadrupolar field.

[18] To support this conclusion, we first order the observed terms in the magnetic induction equation $\partial\mathbf{B}/\partial t = -\nabla \times \mathbf{E}$. Using the generalized Ohm's law we write this as [*Sonnerup*, 1979]

$$\nabla \times \mathbf{E}_{Hall} + \frac{\partial \mathbf{B}}{\partial t} + \mathbf{C}_{res} + \mathbf{C}_{ei} = \nabla \times \frac{\mathbf{v}}{c} \times \mathbf{B} - \mathbf{C}_{ep} \qquad (1)$$

where the contributions labeled $\mathbf{C}$ are due to resistivity (*res*), electron inertia (*ei*), and electron pressure (*ep*), respectively. The terms on the left hand side are written in order of decreasing magnitude as measured in SSX [*Cothran et al.*, 2005], with $|\nabla \times \mathbf{E}_{Hall}|$ larger than other terms on the left hand side of equation (1), including $|\partial\mathbf{B}/\partial t|$, by a factor of $\approx 10^3$. Consequently, the dynamics are quasi-steady and the Hall term must be balanced, approximately, with the sum of motional electric field $-\mathbf{v}/c \times \mathbf{B}$ and electron pressure effects. The nature of this dominant balance is a nontrivial issue of great current interest [*Ishizawa et al.*, 2004], and is probably dependent on position and on plasma parameters, such as plasma beta. It is expected, however, that far from the central neutral line $\mathbf{v}/c \times \mathbf{B}$ effects contribute more to the balance, and that the electron pressure contribution is significant only in a very small layer (of width $\approx$ electron inertial scale) very near the (central) reconnection layer. In any case it is unlikely that electron pressure can completely cancel the Hall contribution everywhere, a point emphasized by *Sonnerup* [1979], and therefore $\mathbf{E}_{Hall}$ is the dominant effect in the region and, presumably, the driver of the observed quadrupolar field.

[19] We now refine this question and ask whether the Hall electric field makes up a large fraction of the total electric field in the region of interest, a necessary condition to argue that collisionless effects produce the quadrupole (Figure 2). The total electric field is estimated in complementary ways: First, the rate of reconnecting flux tubes [*Cothran et al.*, 2003] provides an estimate of $E \sim 100$ V/m near the reconnection zone. Second, measured energetic particles in SSX [*Brown et al.*, 2002] provide an approximate upper bound of 1000 V/m. We use the range 100–1000 V/m as an estimate of the total electric field. The magnitude of the Hall electric field is measured [*Cothran et al.*, 2005] to be large in SSX, more than 1000 V/m during intense reconnection. In Figure 4 we see that the in-plane Hall electric field is as large as several kV/m, while the out-of-plane component (not shown), which balances the reconnection electric field, is 1 kV/m or less. Therefore we conclude that the Hall electric field is a dominant effect in the region where the out-of-plane quadrupolar magnetic field (Figure 2) is measured.

[20] Figure 4 shows the projection of $\mathbf{J} \times \mathbf{B}/(ne)$ onto the 2D reconnection plane defined by Figure 2. This is, apart from density variations, the in-plane Hall electric field. This picture is highly similar to the in-plane total electric field shown by *Wygant et al.* [2005, Figure 5], inferred from Cluster data at a magnetotail crossing. The general pattern is essentially that of a flow associated with 2D reconnection: directed inward on the strong field sides of the X-point in

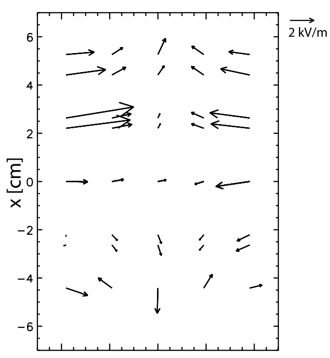

Figure 4. A vector map of the projection of the Hall electric field term $\mathbf{J} \times \mathbf{B}/ne$ (proportional to the Lorentz force) onto the plane of X-point activity shown in Figure 2. The scale is indicated by a 2 kV/m vector (lower left.) This volume force produces flows characteristic of the reconnection process. Using the "right hand rule" one can see that the curl of this quantity exhibits the correct quadrupole pattern, supporting the interpretation that the out-of-plane quadrupolar magnetic field (Figure 2) is due to the Hall electric field, here seen to be comparable to the estimated total electric field of 100–1000 kV/m (see text).

Figure 2, and outward along the weak field sides (between the interacting spheromaks.) The plasma flow is not measured in this SSX setup, but the measured $\mathbf{E}_{Hall}$ is proportional to the Lorentz force, the body force that would drive the expected reconnection flow. Second, the 2D curl of the vector field shown in Figure 4 contributes to $\nabla \times \mathbf{E}_{Hall}$ in the induction equation, and pumps the out-of-plane quadrupolar magnetic field. The active local generation of the quadrupolar magnetic field shown in Figure 2 in fact requires, in the same locations, a quadrupolar driver in $\partial\mathbf{B}/\partial t$, and our measurements support the interpretation that this driving is associated with the Hall electric field. One can readily verify that the predominant sense of rotation of the in-plane $\mathbf{J} \times \mathbf{B}$ shown in Figure 4 has the required symmetry to be interpreted in this way. Therefore we have indication not only of the presence of the quadrupolar magnetic field, but also of its generation by a strong Hall electric field with the required spatial structure.

[21] We believe that this is the first measurement of the generation of the Hall associated quadrupolar field in a laboratory experiment. Preliminary results were presented by *Landreman et al.* [2003]. During evaluation of this paper we became aware of a recent detection of the quadrupolar field by our colleagues in the NSF Center for Magnetic Self Organization, using the MRX experiment, and somewhat different methods [see *Ren et al.*, 2005].

[22] To summarize, when the Hall electric field is significant, the geometry of the reconnection site (Figure 2) must depart from the simple 2D planar symmetry and become 3D. When the Hall electric field is dominant, as measured, electron flow produces a quadrupolar distortion of the magnetic field; this involves, of necessity, an in-plane component of electric current density, the Hall current. One note of caution is that in SSX, an in-plane current can also arise due to the extension into the reconnection zone of the currents that support the toroidal magnetic field. More generally, it is very difficult using any local measurements to entirely rule out influence of distant sources (currents) on the local field (quadrupole). However, we have shown that the driver of the observed out-of-plane quadrupolar distortion can be strongly associated with the quadrupolar pattern induced by the Lorentz force. Therefore local Hall effect driving is implicated, and association of the measured quadrupolar magnetic field distortion with local Hall effect becomes compelling.

[23] **Acknowledgments.** This work was performed under Department of Energy (DOE) grants DE-FG02-00ER54604 and DE-FG02-98ER54490 and the NSF Center for Magnetic Self Organization.

References

Biskamp, D., E. Schwartz, and J. F. Drake (1995), Ion controlled collisionless magnetic reconnection, *Phys. Rev. Lett.*, *75*, 3850.
Brown, M. R. (1999), Experimental studies of magnetic reconnection, *Phys. Plasmas*, *6*, 1717.
Brown, M. R., C. D. Cothran, M. Landreman, D. Schlossberg, and W. H. Matthaeus (2002), Experimental observation of energetic ions accelerated by three-dimensional magnetic reconnection in a laboratory plasma, *Astrophys. J. Lett.*, *577*, L63.
Cothran, C. D., M. Landreman, W. H. Matthaeus, and M. R. Brown (2003), Three dimensional structure of magnetic reconnection in a laboratory plasma, *Geophys. Res. Lett.*, *30*(5), 1213, doi:10.1029/2002GL016497.
Cothran, C. D., M. Landreman, M. R. Brown, and W. H. Matthaeus (2005), Generalized Ohm's law in a 3D reconnection experiment, *Geophys. Res. Lett.*, *32*, L03105, doi:10.1029/2004GL021245.
Hsu, S. C., G. Fiksel, T. A. Carter, H. Ji, R. M. Kulsrud, and M. Yamada (2000), Local measurement of nonclassical ion heating during magnetic reconnection, *Phys. Rev. Lett.*, *84*, 3859.
Ishizawa, A., R. Horiuchi, and H. Ohtani (2004), Two-scale structure of the current layer controlled by meandering motion during steady-state collisionless driven reconnection, *Phys. Plasmas*, *11*, 3579.
Ishizawa, A., and R. Horiuchi (2005), *Phys. Rev. Lett.*, in press.
Ji, H., M. Yamada, S. Hsu, and R. Kulsrud (1998), Experimental test of the Sweet-Parker model of magnetic reconnection, *Phys. Rev. Lett.*, *30*, 3256.
Kornack, T. W., P. K. Sollins, and M. R. Brown (1998), Experimental observation of correlated magnetic reconnection and Alfvénic ion jets, *Phys. Rev. E*, *58*, R36.
Landreman, M. (2003), honors thesis, Swarthmore College, Swarthmore, Pa.
Landreman, M., C. D. Cothran, M. R. Brown, M. Kostora, and J. T. Slough (2003), Rapid multiplexed data acquisition: Application to three-dimensional magnetic field measurements in a turbulent laboratory plasma, *Rev. Sci. Instrum.*, *74*, 2361.
Lukin, V. S., G. Qin, W. H. Matthaeus, and M. R. Brown (2001), Numerical modeling of magnetohydrodynamic activity in the Swarthmore Spheromak Experiment, *Phys. Plasmas*, *8*, 1600.
Ma, Z. W., and A. Bhattacharjee (1996), Fast impulsive reconnection and current sheet intensification due to electron pressure gradients in semi-collisional plasmas, *Geophys Res. Lett.*, *23*, 2955.
Mozer, F. S., S. D. Bale, and T. D. Phan (2002), Evidence of diffusion regions at a subsolar magnetopause crossing, *Phys. Rev. Lett.*, *89*, doi:10.1103/PhysRevLett.89.015002.
Oieroset, M., T. D. Phan, M. Fujimoto, R. P. Lin, and R. P. Lepping (2001), In situ detection of collisionless reconnection in the Earth's magnetotail, *Nature*, *412*, 414.
Phan, T. D., et al. (2000), Extended magnetic reconnection at the Earth's magnetopause from detection of bi-directional jets, *Nature*, *404*, 848.
Priest, E. R., and T. G. Forbes (2000), *Magnetic Reconnection*, Cambridge Univ. Press, New York.
Qin, G., V. S. Lukin, C. D. Cothran, M. R. Brown, and W. H. Matthaeus (2001), Energetic particles and magnetohydrodynamic activity in the Swarthmore Spheromak Experiment, *Phys. Plasmas*, *8*, 1.
Ren, Y., M. Yamada, S. Gerhart, H. Ji, R. Kulsrud, and A. Kuritsyn (2005), Experimental verification of the Hall effect during magnetic reconnection in a laboratory plasma, *Phys. Rev. Lett.*, *95*, doi:10.1103/PhysRevLett.95.055003.
Scudder, J. D., F. S. Mozer, N. C. Maynard, and C. T. Russell (2002), Fingerprints of collisionless reconnection at the separator, I, Ambipolar-Hall signatures, *J. Geophys. Res.*, *107*(A10), 1294, doi:10.1029/2001JA000126.
Shay, M. A., J. F. Drake, R. E. Denton, and D. Biskamp (1998), Structure of the dissipation region during collisionless magnetic reconnection for large systems, *J. Geophys. Res.*, *103*, 9165.
Sonnerup, B. U. O. (1979), Magnetic field reconnection, in *Solar System Plasma Physics*, edited by L. T. Lanzerotti, chap. III.1.2, pp., C. F. Kennel, and E. N. Parker, Elsevier, New York.
Terasawa, T. (1983), Hall current effect on tearing mode instability, *Geophys. Res. Lett.*, *10*, 475.
Wang, X. G., A. Bhattacharjee, and Z. W. Ma (2000), Collisionless reconnection: Effects of Hall current and electron pressure gradient, *J. Geophys. Res.*, *105*, 27,633.
Wygant, J. R., et al. (2005), Cluster observations of an intense normal component of the electric field at a thin reconnecting current sheet in the tail and its role in the shock-like acceleration of the ion fluid into the separatrix region, *J. Geophys. Res.*, *110*, A09206, doi:10.1029/2004JA010708.
Yamada, M., et al. (1997a), Study of driven magnetic reconnection in a laboratory plasma, *Phys. Plasmas*, *4*, 1936.
Yamada, M., et al. (1997b), Identification of Y-shaped and O-shaped diffusion regions during magnetic reconnection in a laboratory plasma, *Phys. Rev. Lett.*, *78*, 3117.

M. R. Brown, C. D. Cothran, and M. Landreman, Department of Physics and Astronomy, Swarthmore College, Swarthmore, PA 19081-1397, USA.
W. H. Matthaeus, Bartol Research Institute, University of Delaware, Newark, DE 19716-4793, USA. (yswhm@bartol.udel.edu)